Journal of The Electrochemical Society, **149** (1) C23-C27 (2002)
0013-4651/2001/149(1)/C23/5/$7.00 © The Electrochemical Society, Inc.

Direct Liquid Injection Metallorganic Chemical Vapor Deposition of ZrO_2 Thin Films Using $Zr(dmae)_4$ as a Novel Precursor

Jeong Seok Na, Dae-Hwan Kim, Kijung Yong, and Shi-Woo Rhee*,z

Laboratory for Advanced Materials Processing, Department of Chemical Engineering, Pohang University of Science and Technology, Pohang 790-784, Korea

A novel liquid Zr precursor with a donor-functionalized alkoxy ligand [$Zr(OCH_2CH_2NMe_2)_4$, $Zr(dmae)_4$] (dmae = dimethylaminoethoxide) has been characterized by thermogravimetry (TG) and differential scanning calorimetry (DSC) analysis, nuclear magnetic resonance, and mass spectrometry. $Zr(dmae)_4$ vaporizes near 320°C and reacts with oxygen at around 310°C under our TG/DSC measurement conditions. The bond strength of Zr-dmae was found to be similar to that of Zr-O^{i}Pr. The ZrO_2 thin films deposited at 300-480°C by a direct liquid injection metallorganic chemical vapor deposition process had a dense and smooth morphology. The film had a weak monoclinic phase in an amorphous background without any other metastable phase such as tetragonal or cubic. The high-frequency (1 MHz) capacitance-voltage curves showed that the flatband voltage (V_{FB}) of the ZrO_2 thin films deposited at 400°C was close to the theoretical value of −0.9 V. The interface trap density near the midgap was found to be less than 1×10^{11} cm^{-2} eV^{-1}, which was calculated by the Terman method.
 [DOI: 10.1149/1.1421605]

Manuscript submitted February 28, 2001; revised manuscript received August 17, 2001. Available electronically November 27, 2001.

Zirconia, ZrO_2, has attracted much interest because of its high dielectric constant (~25), wide energy bandgap (~5 eV), high index of refraction (>2), and good mechanical and chemical stability.[1] The ZrO_2 film can be potentially used as an alternative dielectric material for the storage capacitor in the dynamic random access memory (DRAM).[2] In addition, the related ferroelectric oxide Pb(Zr, Ti)O_3 has a potential application in nonvolatile memories. Recently, ZrO_2 is also investigated as a possible replacement for SiO_2 gate dielectrics. More importantly, it has been reported that ZrO_2 is stable on the Si surfaces.[3,4] The ZrO_2 thin films have been deposited by high-temperature chloride chemical vapor deposition (CVD),[5] low-temperature metallorganic chemical vapor deposition (MOCVD),[6-10] reactive dc magnetron sputtering,[11] and electron-beam evaporation.[12] In particular, MOCVD is a suitable process for the preparation of good quality ZrO_2 thin films by the thermal decomposition of appropriate metallorganic precursors at a relatively low temperature, while the chloride CVD requires a high substrate temperature.

So far the ZrO_2 thin films deposited by MOCVD have been prepared using zirconium oxygenated derivatives such as zirconium alkoxide,[6,7] β-diketonates,[8] fluorinated β-diketonates,[9] and anhydrous nitrates.[10] In particular, zirconium tetrakis(*t*-butoxide) [$Zr(O^tBu)_4$, ZTTB] is the most frequently investigated alkoxide precursor, mainly because it has a high vapor pressure (0.1 Torr at 31°C) and forms films in the temperature range 350-500°C.[9] Unfortunately, this compound is very sensitive to hydrolysis. Zirconium tetrakis(2,2,6,6,-tetramethyl-3,5-heptanedionate) [$Zr(tmhd)_4$], a homoleptic zirconium β-diketonate, has a high thermal stability and allows the optimized growth of ZrO_2 at the substrate temperature greater than 600°C, which is not suitable for the low-temperature CVD process required in the majority of microelectronics applications.

To overcome these problems, a new approach was pursued by using a donor-functionalized alkoxy ligand such as dimethylaminoethoxide (dmae).[13,14] Dmae provides an additional Lewis base site which is able to form the chelate rings. It increases the coordinative saturation relative to an alkoxide precursor such as ZTTB, which contains an unsaturated Zr^{IV} center.

In the present work, we introduced $Zr(dmae)_4$[14] as an alternative zirconium precursor in a direct liquid injection (DLI) for the MOCVD process. We characterized $Zr(dmae)_4$ with thermogravimetry (TG) and differential scanning calorimetry (DSC) analysis, nuclear magnetic resonance (NMR), and mass spectrometry. Also, we investigated the deposition characteristics of the ZrO_2 thin films with a DLI MOCVD using $Zr(dmae)_4$ in an *n*-butyl acetate solvent.

Experimental

Preparation and characterization of Zr(dmae)$_4$.—Zirconium tetra(diethylamine) [$Zr(NEt_2)_4$, 24.68 g, 65 mmol] was added to 150 mL of dry toluene and *N*,*N*-dimethylaminoethanol (26 mL, 260 mmol) was then added slowly to that solution. The mixture was refluxed for 20 h and then cooled. The solvent was removed under a reduced pressure to obtain $Zr(dmae)_4$ as a yellow viscous liquid (yield >90%). ^{1}H NMR (C_6D_6, 300 MHz): δ 4.35 (s, CH_2, 8H), 2.61 (s, CH_2, 8H), 2.30 (s, CH_3, 24H).

To investigate the thermal properties of the sample, TG and DSC analysis (Rheometric) were used in N_2 and O_2 atmospheres at a heating rate of 10°C/min. The cracking patterns of a sample were obtained with a mass spectrometer (JEOL, JMS 700). The sample was ionized by the electron impact (EI) method and the scanned mass range was from 1 to 2000 m/z.

Deposition and characterization of the ZrO_2 films.— The ZrO_2 thin films were deposited using $Zr(dmae)_4$ as a source material by a DLI MOCVD process described in a previous work.[15] Vaporizer temperature was held at 230°C, and the feed line after the vaporizer was held at 240°C to prevent the condensation of the precursor. The susceptor was heated by the tungsten halogen lamps. The reactor pressure was fixed at 1.6 Torr by using the throttle valve between the pump and the reaction chamber. Table I shows the typical deposition conditions. The wafers used were a (100)-oriented p-type Si with the resistivity of 8-12 Ω cm. The modified RCA method, (*i*) dipping in a H_2SO_4:H_2O_2 3:1 solution for 10 min and rinsing with deionized (DI) water, (*ii*) dipping in a HF:H_2O 1:7 solution for 30 s and rinsing with DI water, and (*iii*) blowing with N_2 gas, was used for the predeposition cleaning.

The deposition rate was measured by an α-step 500 surface profiler (Tencor), and the surface morphology was investigated using a scanning electron microscope (SEM, Hitachi S-4200). The crystal structure was analyzed by an X-ray diffractometer (XRD, MacScience M18XHF) with Cu Kα radiation operating at the 30 kV and 40 mA. The depth profile and film composition were investigated by X-ray photoelectron spectroscopy (XPS, PHI 5400 ESCA) with a Al Kα radiation. For electrical characterizations, the metal-insulator-

* Electrochemical Society Active Member.
z E-mail: srhee@postech.ac.kr

Table I. Typical deposition conditions for MOCVD of ZrO_2 thin films.

Substrate	p-type Si(100)
Substrate temperature	300-480°C
Deposition pressure	1.6 Torr
Deposition time	15 min
Gas flow rate	$R[=O_2/(Ar + O_2)] = 0$ (Ar 400 sccm)
	$R = 0.3$ (Ar 280 sccm, O_2 120 sccm)
	$R = 0.5$ (Ar 200 sccm, O_2 200 sccm)
Solution injection rate	0.1 mL/min with 0.1 M precursor solution
Solvent	*n*-butyl acetate
Vaporizer pressure	8 Torr
Vaporizer temperature	230°C

semiconductor (MIS) capacitors were fabricated with the deposited oxides. The aluminum dot electrode, 1.963×10^{-3} cm^2 in area, was deposited by the thermal evaporation through a metallic mask. The capacitance-voltage (C-V) characteristics were analyzed at high frequency (1 MHz) using an HP 4275 multifrequency LCR meter with a sweep voltage range of −4 to +4 V. The interface trap density at the ZrO_2/Si interface was obtained from the C-V data using the Terman method.[16]

Results and Discussion

Characterization of the Zr precursors.—Figure 1 shows a schematic representation of the structure of $Zr(dmae)_4$. Bharara *et al.* synthesized $Zr(dmae)_4$ with zirconium isopropoxide [$Zr(O^iPr)_4$] and dimethylaminoethanol in 1977 for the first time. They revealed that $Zr(dmae)_4$ is a yellow viscous liquid and exhibits monomeric behavior.[14] In this study, we synthesized $Zr(dmae)_4$ with $Zr(NEt)_4$ and dimethylaminoethanol to obtain a high-purity precursor having no mono-, di-, and tris-dimethylaminoethanol derivatives of zirconium, *i.e.*, $Zr(O^iPr)_x(dmae)_{4-x}$ (x = 1-3).

To investigate the thermal properties of $Zr(dmae)_4$, thermogravimetric analysis (TGA) and DSC were performed at a heating rate of 10°C/min. In N_2 atmosphere, an endothermic peak and a rapid weight loss were detected at around 320°C, as shown in Fig. 2a, indicating that the vaporization occurred at around 320°C. Figure 2b shows DSC curves in an oxidizing ambient, which compares the chemical behavior of $Zr(dmae)_4$ with that of $Zr(O^tBu)_4$, a most frequently used alkoxide precursor, and that of $Zr_2(tmhd)_2(O^iPr)_6$. $Zr(O^tBu)_4$ shows an endothermic peak at 170°C, indicating the high volatility of the precursor and then an exothermic peak at about 280°C. $Zr(dmae)_4$ exhibited an exothermic peak at about 310°C, while $Zr_2(tmhd)_2(O^iPr)_6$ showed two exothermic peaks at 315 and 392°C, as shown in Fig. 2b. Based on the report of Lee *et al.*,[17] it is believed that the exothermic peak at about 310°C for both $Zr(dmae)_4$ and $Zr_2(tmhd)_2(O^iPr)_6$ represents the dissociation of the precursor by the oxidation of Zr-dmae and Zr-O^iPr bond, respectively. On the other hand, the exothermic peak at 280°C for $Zr(O^tBu)_4$ and 392°C for $Zr_2(tmhd)_2(O^iPr)_6$ represents the oxidation of Zr-O^tBu and Zr-tmhd bond, respectively. Therefore, it can be expected that the bond strength of Zr-dmae is similar to that of Zr-O^iPr, slightly stronger than that of Zr-O^tBu and lower than that of Zr-tmhd.

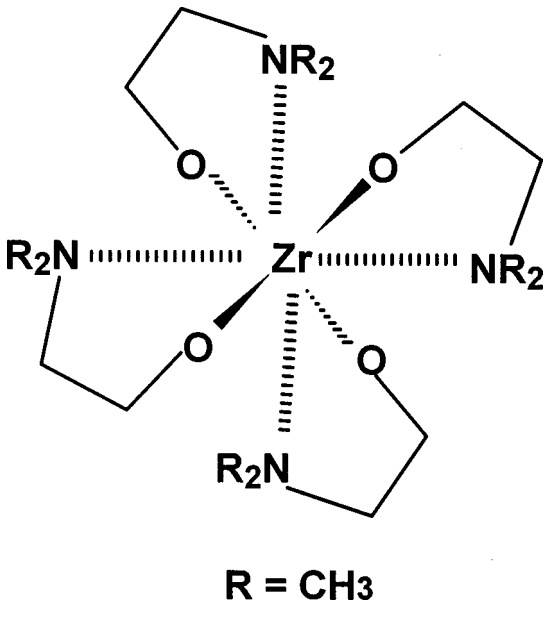

Figure 1. A schematic representation of the structure of $Zr(dmae)_4$.

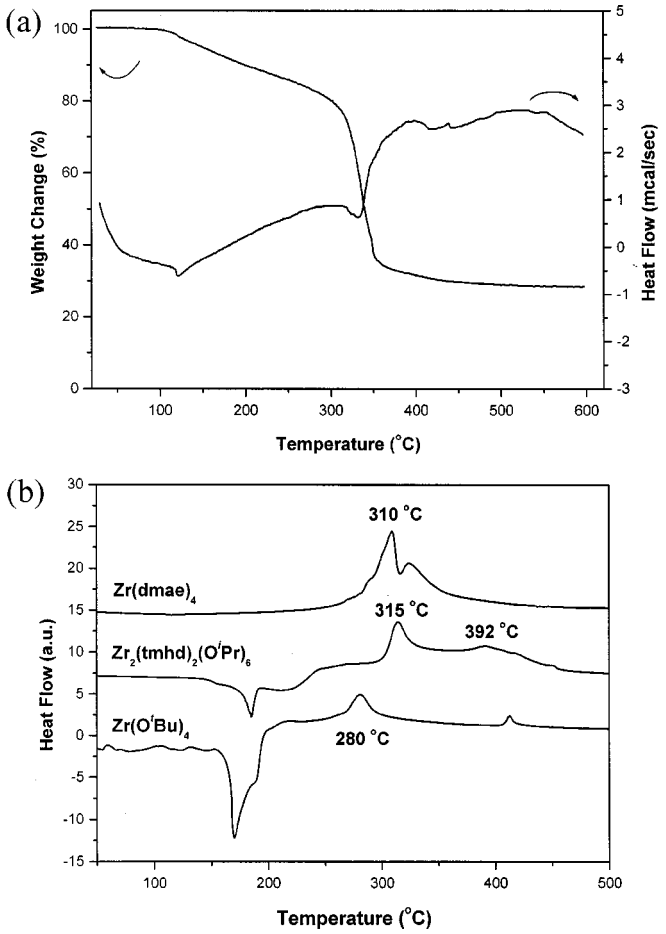

Figure 2. (a) TGA/DSC curve of $Zr(dmae)_4$ in Ar atmosphere. (b) DSC curves of $Zr(dmae)_4$, $Zr_2(tmhd)_2(O^iPr)_6$, and $Zr(O^tBu)_4$ in the oxygen atmosphere. (760 Torr, dT/dt = 10°C/min.)

Mass spectrometry was used to investigate the vaporized species of $Zr(dmae)_4$. The typical mass spectra of $Zr(dmae)_4$ heated at 165°C is shown in Fig. 3. Peaks mainly appeared at positions lower than the molecular weight of $Zr(dmae)_4$ (m/z = 444), and aggregated species of $Zr(dmae)_4$ such as dimer were not detected noticeably. These results might indicate that $Zr(dmae)_4$ exists mainly as a monomer in the gas phase as well as in the liquid state as proposed by Bharara *et al.*[14]

MOCVD of the ZrO_2 thin films.—The ZrO_2 thin films were deposited using flash-vaporized metallorganic precursor solutions with $Zr(dmae)_4$ dissolved in an *n*-butyl acetate solvent. Because the solu-

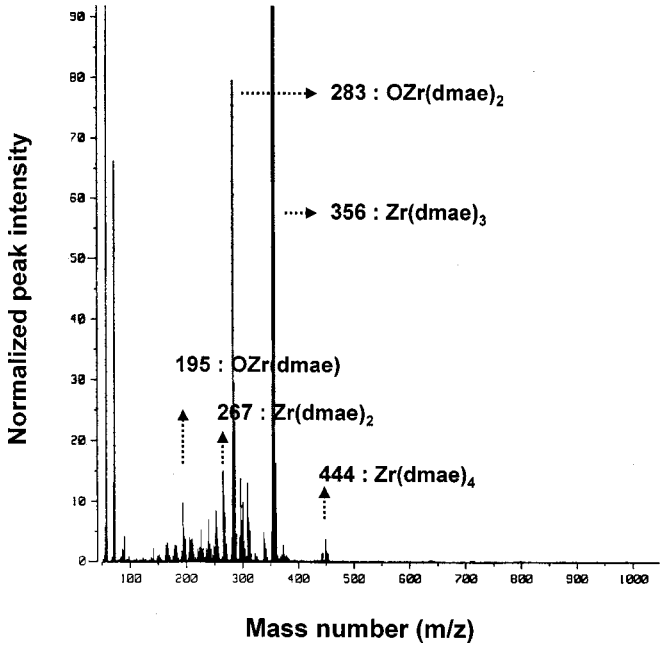

Figure 3. Mass cracking patterns of $Zr(dmae)_4$ at a pressure of 10^{-5} Torr after heating at 165°C.

bility of $Zr(dmae)_4$ is high enough, various solvents can be used. Among various solvents, we selected *n*-butyl acetate that has a high boiling point (bp = 126°C). Also, there is no precipitation in the precursor solution for a month.

Figure 4 shows the Arrhenius plot of the deposition rate as a function of the substrate temperature in the presence of O_2 and the absence of O_2 using $Zr(dmae)_4$ as a new precursor. The variation of the deposition rate with a substrate temperature shows a sharp increase reaching a maximum value at about 360 and 420°C, respectively, in the presence of O_2 and the absence of O_2. The decrease of the growth rate at high temperatures is probably due to the prereaction of precursor molecules with oxygen at high temperatures.[18] In fact, the growth rate of $Zr(dmae)_4$ with O_2 is lower than that of

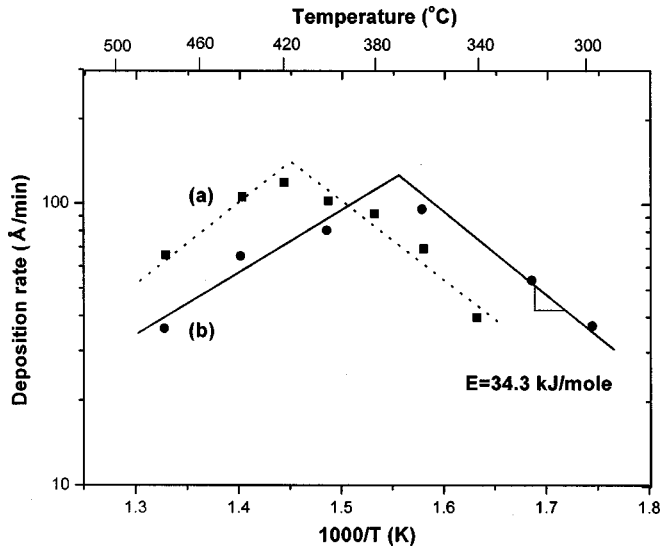

Figure 4. Arrhenius plot of deposition rate as a function of the substrate temperature in (a) the absence of oxygen (Ar 400 sccm) and (b) presence of oxygen with $R[=O_2/(Ar + O_2)] = 0.5$.

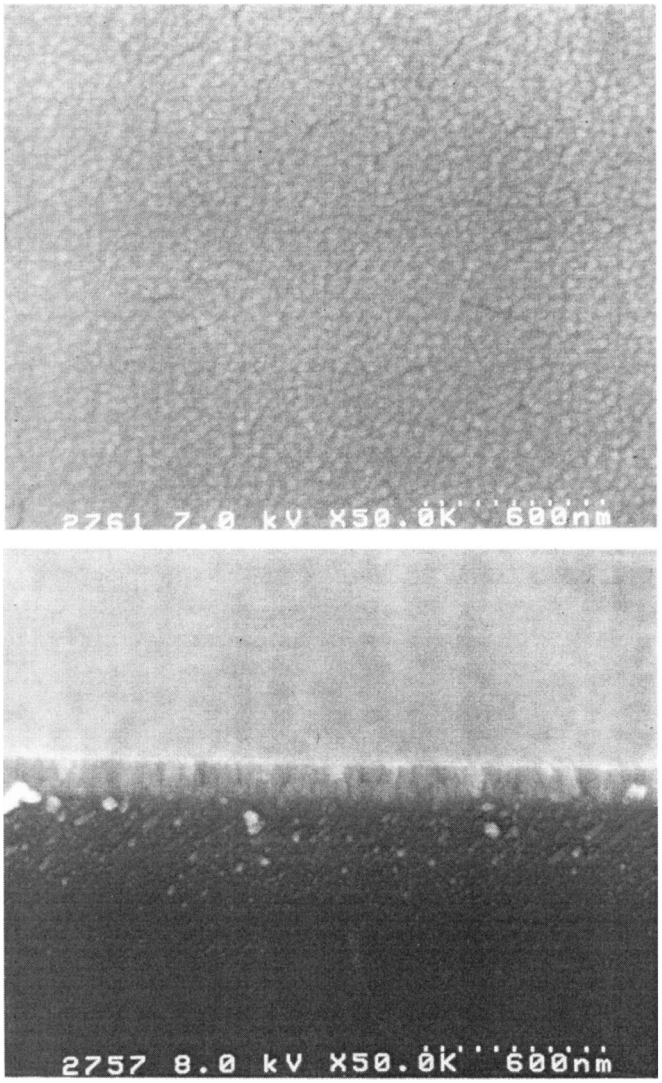

Figure 5. Plan-view (top) and cross-sectional (bottom) SEM micrographs of the ZrO_2 film at a deposition temperature of 400°C with $R = 0.5$.

$Zr(dmae)_4$ without O_2 at temperatures above 380°C. Since we used a cold-wall CVD reactor, the precursor reaction with the reactor wall, which can occur at the high wall temperature, is negligible at the high substrate temperatures. However, more investigations of the decrease of growth rate at high temperatures are required. In the low-temperature region less than 380°C, oxygen has an apparent positive effect on the rate of film growth, but in the higher temperature region above 380°C this effect is negative. The apparent activation energy of the surface chemical reaction calculated from the slope of Fig. 4 is about 34 kJ/mol for both cases. Compared with the reports using other precursors, the rate of ZrO_2 growth has an intermediate value between the value using $Zr(O^tBu)_4$[9] and that using $Zr(tmhd)_4$[10].

Figure 5 shows the SEM images of the ZrO_2 thin film as-deposited at 400°C. The cross-sectional view reveals a uniform film with a fine microstructure, and the plan-view micrograph reveals a fine-grained and dense film surface with an average grain size of 300-400 Å. The grain size was not significantly changed in the substrate temperature range of 340-450°C.

Figure 6 shows XRD patterns of the ZrO_2 thin films. ZrO_2 can adopt three different polymorphs; monoclinic, tetragonal, and cubic phase. Generally, the monoclinic phase is stable below 1170°C. The stability of polymorphs can be affected by the crystallite size or the

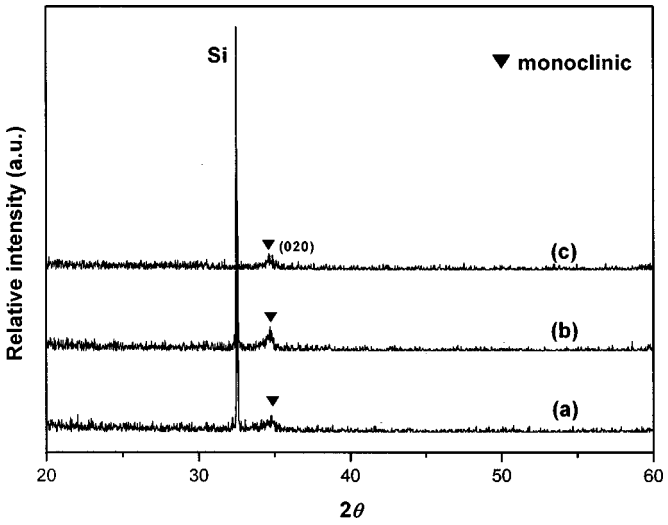

Figure 6. XRD patterns of the ZrO_2 film at various deposition temperatures with $R = 0.5$: (a) 320, (b) 360, and (c) 400°C.

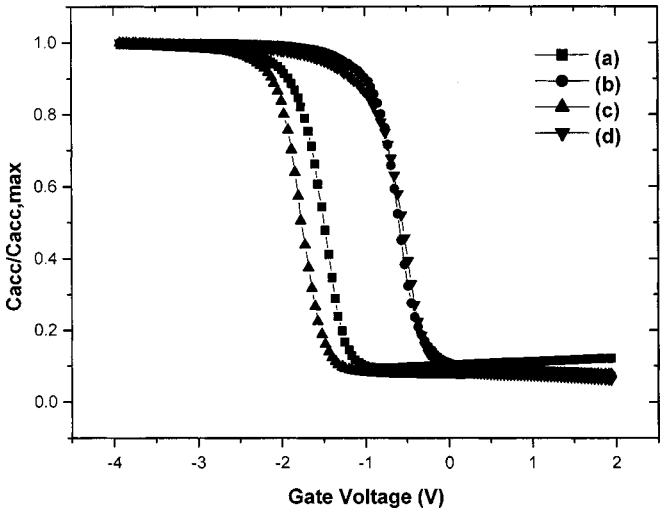

Figure 8. C-V characteristics of ZrO_2 as deposited in an Al/ZrO_2/p-type Si(100) structure at (a) 340°C, $R = 0.3$; (b) 340°C, $R = 0.5$; (c) 400°C, $R = 0.3$; and (d) 400°C, $R = 0.5$.

mechanical strain present in thin films in the form of the residual stress.[19] The films deposited in the temperature range 320-400°C exhibit a weak (020) peak of the monoclinic ZrO_2 in an amorphous background without any other metastable phases in most conditions. When annealed at 700°C for 30 min in air, the phase transformation of ZrO_2 was not observed and only peak intensities of monoclinic phase were slightly increased.

Figure 7 shows the typical XPS depth profile of the as-deposited ZrO_2 film and the variation of the XPS spectra of C 1s for an as-deposited film and a 500°C annealed film in air. The as-deposited ZrO_2 film was found to have an O/Zr ratio of about 1.62 with no significant change after annealing. The nitrogen content was not detected in the films (detection limit ~1 atom %). XPS depth profile shows a uniform concentration distribution of Zr, O, and even carbon impurities through the deposited film. Annealing temperature, 500°C, was selected according to the report of Ma *et al.*[20] The film as-deposited at 400°C has an average carbon content of around 7 atom %, which drops to about 2 atom % by annealing. It is believed that carbon exists as a carbidic state of Zr-C [average binding energy (BE) found: 282.4 eV] in the film. The carbon content of the ZrO_2 film as-deposited at 400°C using $Zr(dmae)_4$ is comparable to about 10 atom % using $Zr(tfacac)_4$ (at 450°C)[2] and 16 atom % using $Zr(acac)_2(hfip)_2$ (at 400°C).[21]

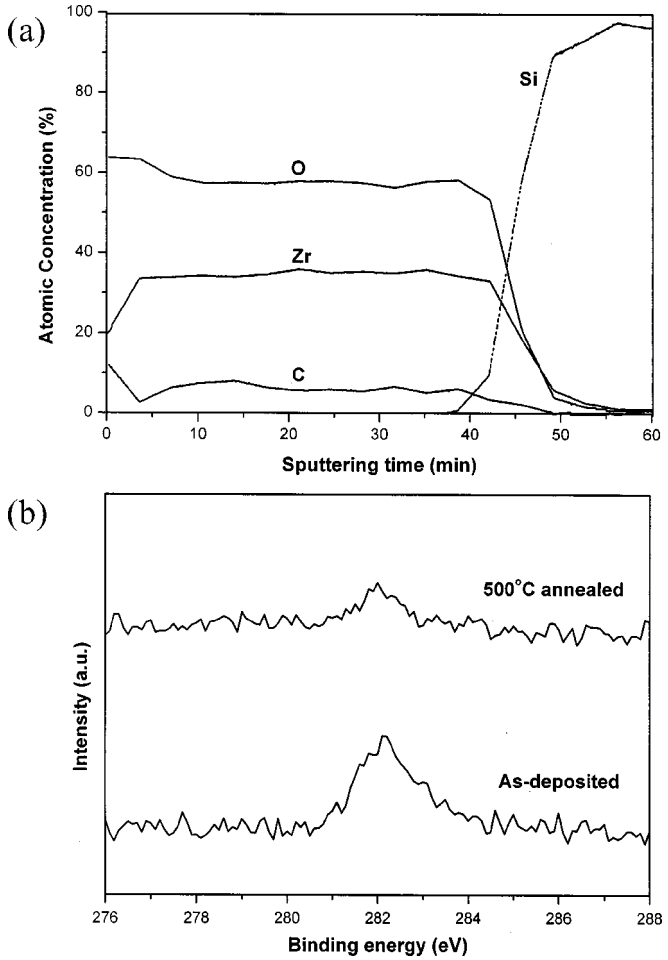

Figure 7. (a) Typical XPS depth profiles of the as-deposited ZrO_2 film with Ar ion sputtering time and (b) XPS spectra of C 1s. (As deposited at 400°C, $R = 0.5$ and annealed at 500°C for 30 min in air.)

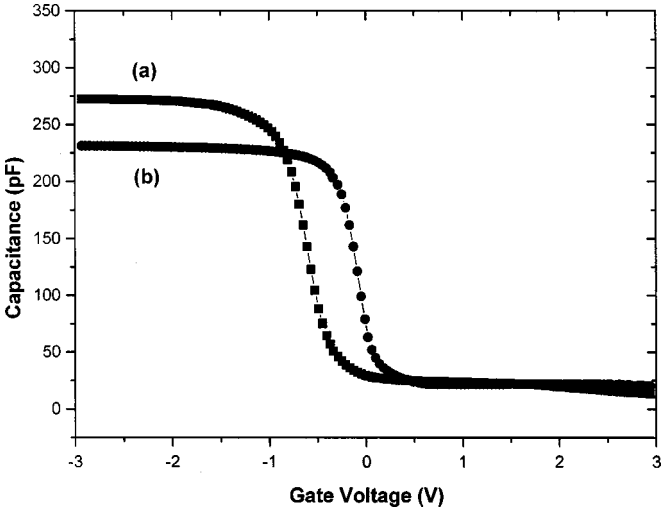

Figure 9. C-V characteristics of (a) as-deposited ZrO_2 film at 400°C, $R = 0.3$, and (b) annealed film at 500°C for 30 min in air.

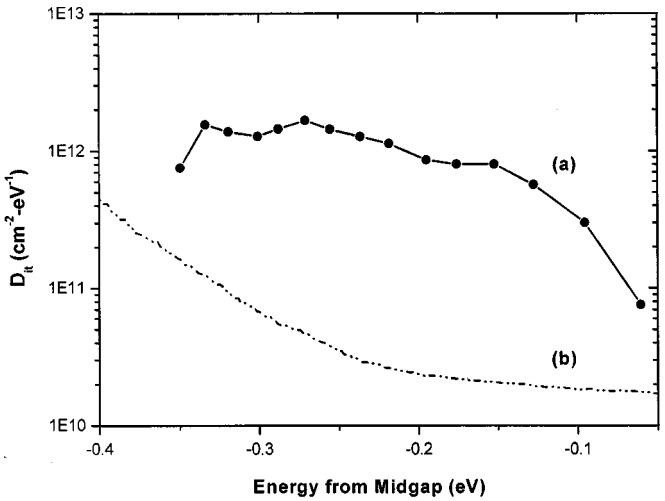

Figure 10. Interface trap density (D_{it}) calculated from 1 MHz C-V curve: (a) $T = 400°C$, $R = 0.5$ and (b) ideal D_{it} on Si⟨100⟩.

Figure 8 shows the typical C-V plot of the MIS device of the Al/ZrO_2/p-type Si(100) structure measured at a high frequency of 1 MHz. From the accumulation capacitance of the MIS structure, the relative dielectric constant of the as-deposited ZrO_2 thin films is estimated to be in the range 15-20. As shown in Fig. 8, the flatband voltage V_{FB} of the ZrO_2 films increases with the increasing deposition temperature from 340 to 400°C, implying an increase of the negative charges in the Zr thin films.[22] The ideal flatband voltage of the Al/ZrO_2/p-type Si is about −0.9 V, which is ϕ_{ms}, the difference in work function between Al and Si. The flatband voltage (V_{FB}) of the ZrO_2 thin films deposited at 400°C is found to be close to this value.

Figure 9 shows the C-V characteristics of the as-deposited ZrO_2 film and the annealed film at 500°C for 30 min in air. It is shown that the accumulation capacitance of the ZrO_2 film decreases by annealing due to the growth of silicon dioxide or Zr silicate at the ZrO_2/Si interface and the crystallization of ZrO_2 film. This behavior was also observed in other literatures.[23,24]

An interface trap density D_{it} can be measured by a high-frequency method developed by Terman.[16] Figure 10 shows both the experimental and the ideal C-V curves for the as-deposited ZrO_2 thin film at 400°C, $O_2/(Ar + O_2) = 0.5$. An interface trap density near the midgap was found to be less than 1×10^{11} cm^{-2} eV^{-1}, which is close to the ideal interface trap density on Si⟨100⟩. The results from Fig. 8-10 demonstrate that good electrical properties in both the bulk and interface regions of the ZrO_2/Si system are obtained for the films grown at 400°C by MOCVD using $Zr(dmae)_4$ as a newly developed precursor.

Conclusions

A liquid Zr precursor [$Zr(OCH_2CH_2NMe_2)_4$, $Zr(dmae)_4$] has been characterized. The precursor vaporizes near 320°C and reacts with oxygen at around 310°C under our TG/DSC measurement conditions. The bond strength of Zr-dmae is similar to that of Zr-O^{i}Pr and stronger than that of Zr-O^{t}Bu. The ZrO_2 films deposited at 300-480°C by a DLI MOCVD process showed a dense and smooth morphology. The film had a weak monoclinic phase in an amorphous background without any other metastable phases. The flatband voltage of the ZrO_2 thin films deposited at 400°C was close to the theoretical value of −0.9 V. The interface trap density near the midgap was found to be less than 1×10^{11} cm^{-2} eV^{-1}. It is thought that $Zr(dmae)_4$ is a useful candidate among the Zr sources for the deposition of the ZrO_2 thin films at the temperature range used here.

Acknowledgment

This work is partly financed by the Consortium of Semiconductor Advanced Research (project no. 00-B6-C0-00-09-00-01).

Pohang University of Science and Technology assisted in meeting the publication costs of this article.

References

1. W. B. Blumenthal, *The Chemical Behavior of Zirconium*, p. 159, Van Nostrand Company, Inc., Princeton, NJ (1958).
2. J. Shappir, A. Anis, and I. Pinsky, *IEEE Trans. Electron Devices*, **ED-33**, 442 (1986).
3. R. Beyers, *J. Appl. Phys.*, **56**, 147 (1984).
4. K. J. Hubbard and D. G. Schlom, *J. Mater. Res.*, **11**, 2757 (1996).
5. R. N. Tauber, A. C. Dumbri, and R. E. Caffrey, *J. Electrochem. Soc.*, **118**, 747 (1971).
6. D. C. Bradley, *Chem. Rev.*, **89**, 1317 (1989).
7. B. J. Gould, L. M. Povey, M. E. Pemble, and W. R. Flavell, *J. Mater. Chem.*, **4**, 1815 (1994).
8. M. Balog, M. Shieber, M. Michiman, and S. Patai, *Thin Solid Films*, **47**, 109 (1977).
9. M. Balog, M. Shieber, M. Michiman, and S. Patai, *J. Electrochem. Soc.*, **126**, 1203 (1979).
10. D. G. Colombo, D. C. Gilmer, V. G. Young, S. A. Cambell, and W. L. Gladfelter, *Chem. Vap. Deposition*, **4**, 220 (1998).
11. W. J. Qi, R. Nieh, B. H. Lee, L. Kang, Y. Jeon, K. Onishi, T. Ngai, S. Banerjee, and J. C. Lee, *Tech. Dig. Int. Electron Devices Meet.*, **1999**, 145.
12. M. Morita, H. Fukumoto, T. Imura, and Y. Osaka, *J. Appl. Phys.*, **56**, 2407 (1985).
13. W. A. Herrmann, N. W. Huber, and O. Runte, *Angew. Chem. Int. Ed. Engl.*, **34**, 2187 (1995).
14. P. C. Bharara, V. D. Gupta, and R. C. Mehrotra, *Synth. React. Inorg. Met.-Org. Chem.*, **7**, 537 (1977).
15. J.-H. Lee, J.-Y. Kim, J.-Y. Shim, and S.-W. Rhee, *J. Vac. Sci. Technol. A*, **17**, 3033 (1999).
16. L. M. Terman, *Solid-State Electron.*, **5**, 285 (1962).
17. J.-H. Lee, J.-Y. Kim, and S.-W. Rhee, *Electrochem. Solid-State Lett.*, **2**, 622 (1999).
18. A. C. Jones, T. J. Leedham, P. J. Wright, M. J. Crosbie, K. A. Fleeting, D. J. Otway, P. O'Brien, and M. E. Pemble, *J. Mater. Chem.*, **8**, 1773 (1998).
19. R. C. Garvie, *J. Phys. Chem.*, **68**, 1238 (1965).
20. Y. Ma, Y. Ono, L. Stecker, D. R. Evans, and S. T. Hsu, *Tech. Dig. Int. Electron Devices Meet.*, **1999**, 149.
21. M. Morstein, I. Pozsgai, and N. D. Spencer, *Chem. Vap. Deposition*, **5**, 151 (1999).
22. C. H. Ling, J. Bhaskaran, W. K. Choi, and L. K. Ah, *J. Appl. Phys.*, **77**, 6350 (1995).
23. H. Fukumoto, M. Morita, and Y. Osaka, *J. Appl. Phys.*, **65**, 5210 (1989).
24. T. S. Kalkur and Y. C. Lu, *Thin Solid Films*, **207**, 193 (1992).